

and *Band Structure of Semiconductors* (Pergamon, New York, 1968), p. 25.

<sup>12</sup>Y. S. Park and J. R. Schneider, *J. Appl. Phys.* **39**, 3049 (1968).

<sup>13</sup>H. R. Phillip and H. Ehrenreich, in *Semiconductors and Semimetals*, edited by R. Willardson and A. Beer (Academic, New York, 1967), Vol. 3, p. 93.

<sup>14</sup>G. Heiland, E. Mollwo, and F. Stockmann, in *Solid State Physics*, edited by F. Seitz and D. Turnbull (Academic, New York, 1959), Vol. 8, p. 191.

<sup>15</sup>D. Stukel *et al.*, *Phys. Rev.* **179**, 740 (1969).

<sup>16</sup>A. W. Blackstock, R. D. Birkhoff, and M. Slater,

*Rev. Sci. Instr.* **26**, 274 (1955).

<sup>17</sup>L. Marton and J. A. Simpson, *Rev. Sci. Instr.* **29**, 567 (1958).

<sup>18</sup>H. Mendlowitz, *Rev. Sci. Instr.* **29**, 701 (1958).

<sup>19</sup>G. A. Harrower, *Rev. Sci. Instr.* **26**, 852 (1955).

<sup>20</sup>J. Hubbard, *Proc. Phys. Soc. (London)* **A68**, 976 (1955).

<sup>21</sup>C. B. Wilson, *Proc. Phys. Soc. (London)* **76**, 481 (1960).

<sup>22</sup>Y. S. Park *et al.*, DESY Report No. 7019, 1970 (unpublished).

PHYSICAL REVIEW B

VOLUME 1, NUMBER 12

15 JUNE 1970

## Self-Consistent Energy Bands and Related Properties of Boron Phosphide

D. J. Stukel

*Aerospace Research Laboratories, Wright-Patterson Air Force Base, Ohio 45433*

(Received 29 December 1969)

A first-principles self-consistent orthogonalized-plane-wave energy-band calculation has been performed for cubic boron phosphide (BP) using a nonrelativistic formalism and Slater's free-electron exchange approximation. These are the first fully self-consistent energy-band solutions reported for BP. The imaginary part of the dielectric constant, spin-orbit splittings, effective masses, deformation energies, and the x-ray form factors (Fourier transforms of the electron charge density) have been calculated. The theoretical results are compared with the available experimental data.

### I. INTRODUCTION

Boron phosphide (BP) is a group III-V compound semiconductor. Scientific interest in this compound is stimulated by its potential for solid-state devices; however, many of the important basic physical properties have not been well established. Crystalline BP, as a substance for semiconductor compounds, has advantages such as a high melting point, chemical inertness, and high mechanical hardness.

Cubic BP has a melting point greater than 3000 °C but decomposes into B<sub>6</sub>P and P<sub>2</sub> at much lower temperatures. Hence, the customary methods of crystal growing are not applicable. However, single crystals of sufficient size and purity for optical and electrical measurements have been prepared. Methods of growing crystalline BP have been reviewed by Williams.<sup>1</sup> BP crystallizes in the fcc zinc-blende structure with a lattice parameter of 4.538 Å.<sup>2,3</sup> BP shows both physical and chemical properties that differ from the general trend of the III-V family. BP is quite inert chemically. It has a hardness about equal to that of SiC.<sup>4</sup>

The purpose of this paper is to report for BP a theoretical calculation of the band structure, the

imaginary part of the dielectric constant ( $\epsilon_2$ ) derived from the theoretical bands, spin-orbit splittings, effective masses, deformation energies, and the form factors (the Fourier transforms of the electron charge density).

In the past couple of years, a great deal of success has been attained in calculating the energy band structures of group III-V, II-VI, and IV compounds using an unadjusted first-principles self-consistent orthogonalized-plane-wave (SCOPW) model developed here at the Aerospace Research Laboratories. The (SCOPW) programs used to calculate the electronic band structure have given surprisingly good one-electron band energies for tetrahedrally bonded compounds when Slater's exchange is used.<sup>5-11</sup>

### II. CALCULATIONAL DETAILS

#### A. Self-Consistent OPW model

The orthogonalized-plane-wave (OPW) method of Herring<sup>12</sup> is used to calculate the electron energies. In the SCOPW model,<sup>5,6</sup> the electronic states are divided into tightly bound core states and loosely bound valence states. The core states must have negligible overlap from atom to atom. They are

calculated from a spherically symmetrized crystalline potential.

The valence states must be well described by a modified Fourier series

$$\psi_{k_0}(r) = \sum_{\mu} B_{\mu} (1/\sqrt{\Omega_0}) e^{i\vec{k}_{\mu} \cdot r} - \sum_a e^{i\vec{k}_{\mu} \cdot \vec{R}_a} \sum_{\alpha} A_{\alpha\mu}^a (\psi - \psi_a),$$

where  $\vec{k}_{\mu} = \vec{k}_0 + \vec{K}_{\mu}$ ,  $\vec{k}_0$  locates the electron within the first Brillouin zone,  $\vec{K}_{\mu}$  is a reciprocal-lattice vector,  $\vec{R}_a$  is an atom location,  $\psi_c$  is a core wave function, and  $\Omega_0$  is the volume of the crystalline unit cell. The coefficients  $A_{\alpha\mu}^a$  are determined by requiring that  $\psi_{k_0}(r)$  be orthogonal to all core-state wave functions. The variation of  $B_{\mu}$  to minimize the energy then results in the valence one-electron energies and wave functions.

The dual requirements of no appreciable core overlap and the convergence of the valence wave-function expansion with a reasonable number of OPW's determine the division of the electron states into core and valence states. For B, the 2s and 2p states (for P, the 3s and 3p states) are taken as the valence states. OPW series convergence is discussed in Sec. II B.

The calculation is self-consistent in the sense that the core and valence wave functions are calculated alternately until neither changes appreciably. The Coulomb potential due to the valence electrons and the valence charge density are both spherically symmetrized about each inequivalent atom site. With these valence quantities frozen, new core wave functions are calculated and iterated until the core wave functions are mutually self-consistent. The total electronic charge density is calculated at 650 crystalline mesh points covering  $\frac{1}{24}$  of the unit cell, and the Fourier transform of  $\rho(r)^{1/3}$  is calculated. The new crystal potential is calculated from the old valence charge distribution and new core charge distribution. Then new core valence orthogonality coefficients  $A_{\alpha\mu}^a$  are calculated. The iteration cycle is then completed by the calculation of new valence energies and wave functions. The iteration process is continued until the valence one-electron energies change less than 0.01 eV from iteration to iteration.

The appropriate charge density to use for both the self-consistent potential calculation and the form-factor calculation is the average charge density of all the electrons in the Brillouin zone. In the present self-consistent calculations, this average is approximated by a weighted average over electrons at the  $\Gamma$ , X, L, and W high-symmetry points of the Brillouin zone shown in Fig. 1. The weights are taken to be proportional to the volumes within the first Brillouin zone closest to each high-symmetry point. The adequacy of this approximation has been tested and the error in the energy eigenvalues due to this approximation has been shown

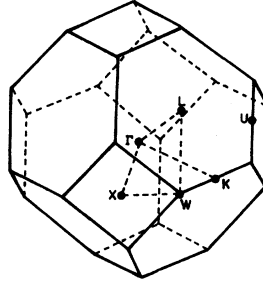


FIG. 1. Zinc-blende Brillouin zone with high-symmetry points labeled.

to be less than 0.1 eV.<sup>10</sup>

The present self-consistent model neglects correlation effects and approximates the complicated Hartree-Fock exchange potential by a term proportional to the electron charge density to the  $\frac{1}{3}$  power. The best known exchange potentials are Slater's<sup>13</sup>

$$V_{xS} = -6[(3/8\pi)\rho(r)]^{1/3}$$

and Kohn and Sham's<sup>14</sup> and Gaspar's<sup>15</sup>

$$V_{xKSG} = -4[(3/8\pi)\rho(r)]^{1/3}.$$

When calculating the energy band structure of tetrahedrally bonded semiconductors with our SCOPW model, we have found that Slater's exchange always gives results that agree most closely with experiment.<sup>11</sup> The many-body work of Hedin, Lundqvist, and co-workers supports the choice of Slater's exchange and shows why Slater's exchange gives good excitation energies.<sup>16</sup> To indicate which transitions are most sensitive to the value of the exchange constant, both the Slater and Kohn-Sham-Gaspar energies are tabulated in Table I for selected high-symmetry points.

In order to calculate the absorptive part of the dielectric constant  $\epsilon_2$ , a pseudopotential fit is made to the relevant energy levels at the  $\Gamma$ , X, L, and W points. The pseudopotential technique is then used to calculate energy differences and transition matrix elements throughout the Brillouin zone.<sup>17</sup> In our experience, this procedure gives the  $\epsilon_2$  peaks at the correct energies. However, the relative peak heights do not match experiment because of their dependence upon the poor pseudopotential wave functions, and because of complicated electron-hole and electron-phonon interactions which are ignored in our model.

One way of taking relativistic effects into account within the framework of nonrelativistic band calculations is with first-order perturbation theory. The perturbing Hamiltonian obtained for the spin-orbit splitting is

$$\hat{H}_{so} = -\frac{1}{4}iq^2\hat{\sigma} \cdot [\vec{\nabla}V(r) \times \vec{\nabla}],$$

where  $V(r)$  is the potential,  $\hat{\sigma}$  is the Pauli spin operator, and  $q$  is the fine structure constant. The

TABLE I. Self-consistent energy eigenvalues for cubic BP based on a lattice constant of 4.538 Å, the Slater and Kohn-Sham exchanges, and on a four-point ( $\Gamma$ ,  $X$ ,  $L$ , and  $W$ ) zone sampling. 459 and 411 OPW's were used at  $\Gamma$  and a comparable number of OPW's at  $X$ ,  $L$ , and  $W$ . The zero of energy has been placed at the top of the valence band ( $\Gamma_{15v}$ ). All entries are in eV.

Level	Slater exchange		Kohn-Sham
	459 OPW's	411 OPW's	exchange 459 OPW's
$\Gamma_{1c}$	6.80	6.77	7.27
$\Gamma_{15c}$	3.63	3.64	3.11
$\Gamma_{15v}$	0.0	0.0	0.0
$\Gamma_{1v}$	-15.30	-15.31	-15.67
$X_{1c}$	2.24	2.25	1.16
$X_{3c}$	1.93	1.93	0.94
$X_{5v}$	-3.95	-3.95	-4.29
$X_{3v}$	-8.44	-8.47	-8.71
$X_{1v}$	-10.70	-10.70	-10.76
$X_{1c}-X_{5v}$	6.19	6.20	5.47
$X_{3c}-X_{5v}$	5.88	5.88	5.23
$L_{3c}$	5.17	5.18	4.40
$L_{1c}$	3.80	3.80	3.60
$L_{3v}$	-1.71	-1.72	-1.82
$L_{1v}$	-8.73	-8.75	-9.31
$L_{1v}$	-12.16	-12.17	-12.26
$L_{3c}-L_{3v}$	6.88	6.90	6.22
$L_{1c}-L_{3v}$	5.51	5.52	5.42
$W_{3c}$	7.04	7.04	6.21
$W_{2c}$	6.08	6.10	5.13
$W_{3v}$	-5.11	-5.11	-5.76
$W_{2v}$	-5.36	-5.37	-6.00
$W_{1v}$	-7.97	-8.00	-8.10
$W_{4v}$	-10.49	-10.49	-10.46
$W_{2c}-W_{3v}$	11.19	11.21	10.86

$\Gamma_{15v}$  SCOPW valence wave functions are used in this calculation.

### B. OPW Series Convergence

A major problem involved in an OPW calculation of a compound which has a constituent from the first row of the Periodic Table such as B is the very slow convergence of the OPW series expansion of the valence and conduction wave functions. In the OPW expansion, all  $k$  vectors are used which have magnitudes smaller than some value  $k_{\max}$ . The minimum distance that can be defined by the plane-wave terms in the OPW series is thus roughly

$$d_{\min} \approx \frac{1}{2} \lambda_{\min} = \pi/k_{\max} = a/2(m^2 + n^2 + l^2)^{1/2},$$

where  $a$  is the lattice constant and  $(m, n, l)$  are integers defining the largest  $k$  vector. The dependence of the BP valence- and conduction-band energies upon  $d_{\min}$  is shown for two different OPW models in Figs. 2 and 3. In Fig. 2, Herman's overlapping free-atomic-potential model<sup>18</sup> is used in which the potential is calculated from free-atom charge densities which are packed in the crystal lattice. In Fig. 3, SCOPW results are presented for different  $d_{\min}$ . For both figures, the B and P core charge densities [ $4\pi r^2 \rho(r)$ ] are also shown.

It has been shown that the series convergence depends upon two factors.<sup>19</sup> One is the relative core size of anion and cation.  $d_{\min}$  depends upon the lattice constant which depends upon the sum of anion and cation core sizes. The penetration into the smaller core is thus least when the core size ratio is most extreme. The second factor involves the presence or absence of core wave functions in

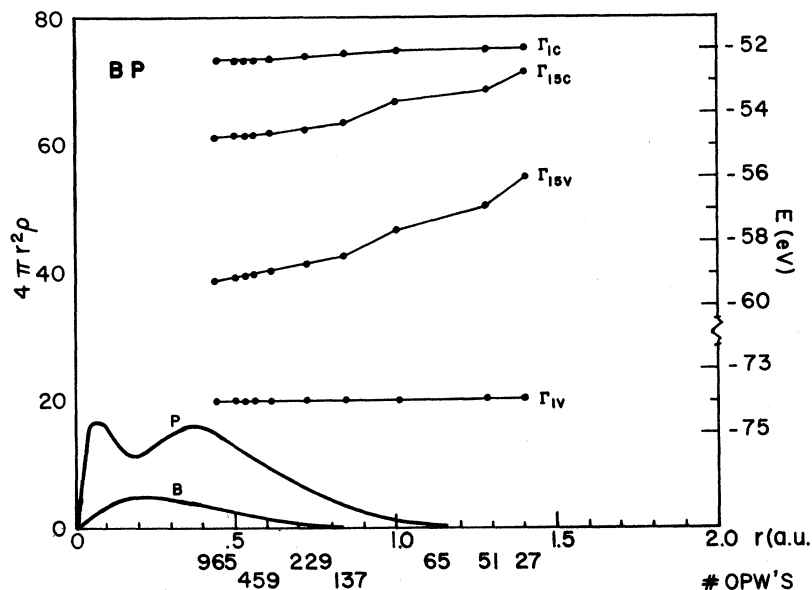


FIG. 2. Convergence study of non-self-consistent energy levels at  $\Gamma$  point in cubic BP.

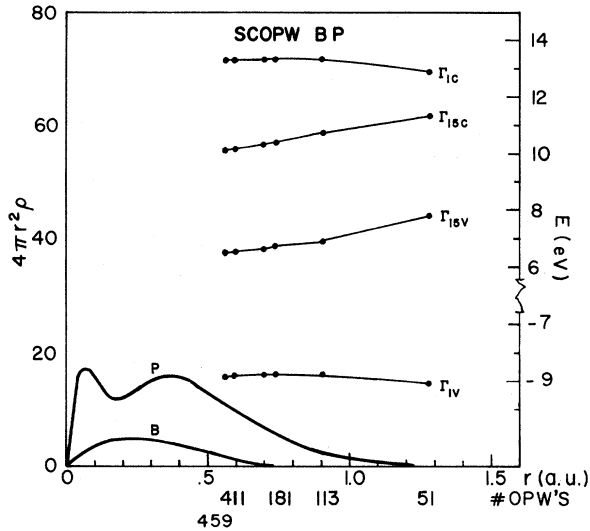


FIG. 3. Convergence study of SCOPW energy levels at  $\Gamma$  point in cubic BP.

symmetrized OPW's. If no core wave functions are present in an OPW expansion, it becomes a pure plane-wave expansion (Fourier series) with consequently poorer convergence. B has no  $p$  states in the core, and thus the  $\Gamma_{15v}$  wave function contains no B core states to aid convergence. The only saving factor is that  $\Gamma_{15v}$  convergence depends much more critically upon penetration into the anion than upon cation penetration. But it can be seen from the figures that convergence of the energies is still not complete by 965 OPW's. This lack of convergence can also be seen more quantitatively in Table II where SCOPW energies are given when 411 and 459 OPW's were used. In going from 411 to 459 OPW's, the  $\Gamma_{1v}$ ,  $\Gamma_{15v}$ ,  $\Gamma_{15c}$ , and  $\Gamma_{1c}$  changed by 0.03, 0.04, 0.05, and 0.01 eV, respectively. We estimate a maximum uncertainty of 0.3 eV in our 459 SCOPW results owing to lack of OPW convergence.

### III. RESULTS

In the SCOPW model, the input data consist of the crystal symmetry, the nuclear charge of the cation and anion, the lattice constant, and the exchange constant. In these calculations the lattice constant used was 4.538 Å.<sup>2,3</sup> Self-consistent calculations were also made with a lattice constant of 4.528 Å to determine the effects of pressure. Slater's exchange was used, since experience with tetrahedral semiconductors has shown that when it is used, one obtains good agreement with experiment.

The energy bands based on Slater's exchange, a lattice constant of 4.538 Å, and 459 OPW's at  $\Gamma$  (and a comparable number of OPW's at X, L, and

W), are given in Fig. 4. The energy eigenvalues are given in the second column of Table I. The calculated band structure is quite similar to that of other III-V compounds. The theoretical calculations yielded an indirect gap  $\Delta_{1c}^m - \Gamma_{15v}$  of 1.80 eV. The minimum in the conduction band occurs 0.81 of the distance from the  $\Gamma$  to the X point. The next lowest minimum occurs at the  $\Gamma$  point.

Stone and Hill<sup>20</sup> made the first optical transmission measurements on amorphous BP. A large abrupt decrease in the transmittance of 6.0 eV was taken to indicate a band gap of that width even though a small inflection occurred in their data at 2.0 eV. However, now it has been established that the experimental band-gap energy is only about 2 eV. The first report of this lower value was by Archer, Koyama, Loebner, and Lucas<sup>21</sup> who obtained agreement within 50 meV from room-temperature measurements of optical absorption, injection electroluminescence, and photoelectric response of surface barrier contacts. At about the same time Wang, Cardona, and Fischer<sup>3</sup> determined from transmission measurements that the fundamental absorption edge of BP is near 2 eV and caused by indirect transitions from the  $k=0$  top of the valence band to a conduction-band minimum

TABLE II. Self-consistent energy eigenvalues for BP based on four-point zone sampling, Slater's exchange, 459 OPW's, and a lattice constant of 4.538 Å are given in column 2. The changes in the eigenvalues when self-consistency was obtained at 4.528 Å are given in column 3. The resulting deformation energies appear in column 4. The energies are in eV. Deformation energies (DE) are in eV per unit dilation.

Level	Energy (4.538 Å)	$E_{4.528} - E_{4.538}$	DE
$\Gamma_{1v}$	- 8.830	0.039	5.9
$\Gamma_{15v}$	6.471	0.096	14.5
$\Gamma_{15c}$	10.102	0.103	15.6
$\Gamma_{1c}$	13.275	0.193	29.2
$X_{1v}$	- 4.231	0.075	11.3
$X_{3v}$	- 1.969	0.060	9.1
$X_{5v}$	2.521	0.072	10.9
$X_{3c}$	8.397	0.087	13.2
$X_{1c}$	8.707	0.089	13.5
$L_{1v}$	- 5.689	0.064	9.7
$L_{1v}$	- 2.256	0.050	7.6
$L_{3v}$	4.759	0.087	13.2
$L_{1c}$	10.269	0.135	20.4
$L_{3c}$	11.643	0.101	15.3
$W_{4v}$	- 4.019	0.079	12.0
$W_{1v}$	- 1.499	0.066	10.0
$W_{2v}$	1.109	0.060	9.1
$W_{3v}$	1.364	0.059	8.9
$W_{2c}$	12.552	0.095	14.4
$W_{3c}$	13.516	0.111	16.8

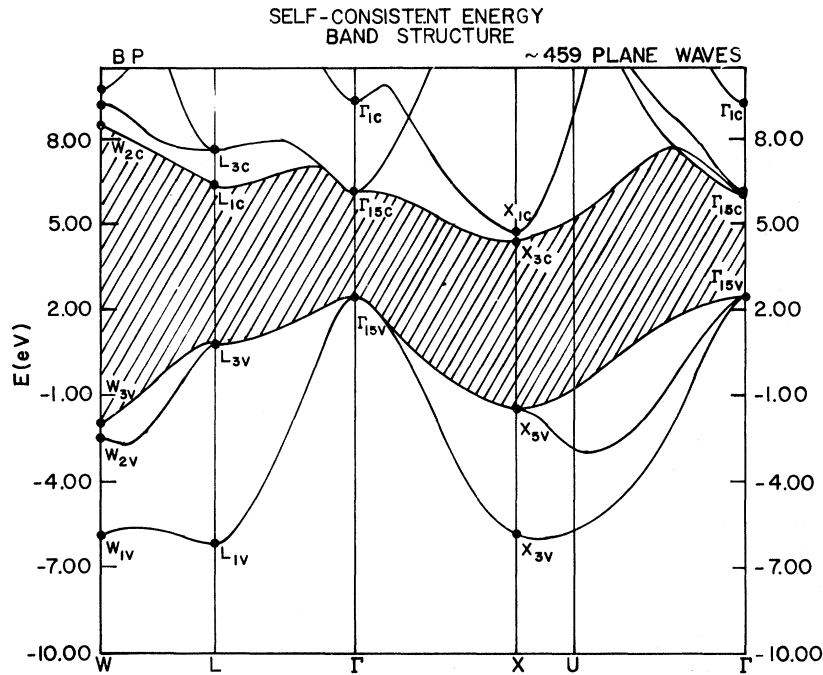


FIG. 4. SCOPW energy band structure of BP. The solid dots denote SCOPW energy levels. The solid lines were obtained by fitting a pseudopotential-type interpolation scheme to the SCOPW energy levels.

at the X point. They attributed this small value of the energy gap to an extremely small ionicity. Fomichev, Zhukova, and Polushina<sup>22</sup> obtained a value of  $2.0 \pm 0.2$  eV for the band gap of BP by ultrasoft x-ray spectroscopy.

In the literature, one finds completely different empirical predictions of the band gap of BP. For example, Manca,<sup>23</sup> on the basis of the correlation between the value of the energy gap and the single-bond energy, predicted a band gap of 4.2 eV. Sclar<sup>24</sup> predicted a gap of 6.2 eV based on an empirical formula connecting the energy gap with the ionic and covalent atomic radii of the constituent elements. However, Stearns,<sup>25</sup> in considering these predictions, called attention to the fact that the III-V compounds are ordinarily more ionic than their group-IV analogs, but just the opposite is true of borides. Starting from these considerations, he predicted a band gap of 2.1 eV.

To calculate the effects of hydrostatic pressure on the band energies, we iterated to self-consistency using a lattice constant of 4.528 Å in addition to the equilibrium lattice constant of 4.538 Å. The results are presented in Table II. The deformation energies given in column 4 of Table II are defined as

$$DE = \frac{\delta E}{\delta V/V} = - \frac{\delta E}{3\delta a/a}$$

and are given in units of eV per unit dilation.  $a$  is the lattice constant.

The imaginary part of the dielectric constant ( $\epsilon_2$ ) is given in Fig. 5. The locations of some of

the major transitions are also indicated. It should be remembered that the detailed  $\epsilon_2$  shape is unreliable, while the peak positions are much more reliable.

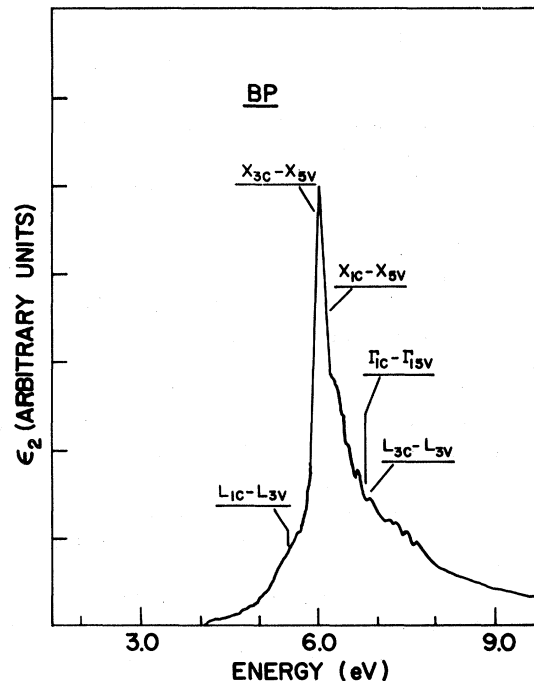


FIG. 5. Theoretical  $\epsilon_2$  curve for BP with the location of the high-symmetry-point transitions shown.

In the theoretical  $\epsilon_2$ , there is only one strong peak which occurs at 6.16 eV. This peak originates in the outer region of the zone. In most zinc-blende II-VI and III-VI compound semiconductors, as well as group-IV semiconductors, there are three peaks. The lowest peak is due to transitions closely related to the  $L_{1c}-L_{3v}$  transitions. The second peak, commonly called the  $X$  peak, is due to transitions in the outer part of the zone,  $U-K$  region. The third peak is due to transitions closely related to the  $L_{3c}-L_{3v}$  transitions. In theoretical calculation of Si, all workers have had difficulty in obtaining the first peak. It has been suggested that this is due to excitonic effects. In a theoretical calculation of AlP, this first peak is barely present as it is in the case of BP. The peak is much more evident in BAs. The third peak in other zinc-blende and diamond semiconductors such as BAs, AlP, AlAs, GaP, GaAs, and Si is much more pronounced than it is in BP.

Wang *et al.* found, at room temperature, the main reflectivity maximum at 6.9 eV, a weak maximum at 5.0 eV and a shoulder at 8.0 eV. They interpreted the main peak as due to  $X$  point transitions, the weak maximum as due to  $\Gamma_{15c}-\Gamma_{15v}$  transitions, and the shoulder as due to  $L_{3c}-L_{3v}$  transitions. Since the  $\epsilon_2$  peak is usually 0.2 or 0.3 of an eV below the reflectivity peak, the theoretical calculation differs from the experimental results by 0.4 or 0.5 of an eV. The weak maximum that Wang *et al.* found at 5.0 eV is probably related to the  $L_{1c}-L_{3v}$  transitions we find theoretical at 5.51 eV. We have no structure that corresponds to the weak shoulder Wang *et al.* found at 8.0 eV. It is possible that part of the difference between theoretical and experimental results can be attributed to the lack of convergence of the wave-function expansions.

The spin-orbit splitting at  $k=0$  of the top  $\Gamma_{15v}$  valence band into  $\Gamma_7$  and  $\Gamma_8$  bands has been found by the use of first-order perturbation theory on the self-consistent Slater  $\Gamma_{15v}$  wave functions to be 0.06 eV.

Effective masses have been calculated for the top valence band at the  $\Gamma$  point and for the bottom conduction band at the  $\Gamma-X$  minimum. For the  $\Gamma_{15v}$  valence band (where spin-orbit splitting has been neglected)  $m_{\Gamma}^*$  is 0.5 for the heavy hole and 0.2 for the light hole for the (1, 1, 1) direction and  $m_{\Gamma}^*$  is 0.3 for both the heavy hole and light hole for the (1, 0, 0) direction. For the conduction-band minimum in the (1, 0, 0) direction, the effective mass in the parallel direction is about 0.9.

In Table III, theoretical Fourier components of the charge density (the x-ray form factors) are given. The Fourier components in the column headed RHF are obtained by the superposition of

TABLE III. Theoretical BP structure factors in electron per crystallographic unit cell. The RHF values are relativistic free-atomic Hartree-Fock results. KS and SI refer to the use of the Kohn-Sham or Slater exchange approximation. SI-RHF (for example) refers to structure factors calculated using SCOPW valence electron densities and RHF free-atomic core densities. 459 OPW's were used in the wave-function expansion.

$hkl$	RHF	KS	KS-RHF	SI	SI-RHF
111	43.63	44.45	44.52	45.41	45.34
200	29.55	29.23	29.31	29.85	29.72
220	41.54	41.26	41.46	41.94	41.79
311	32.27	31.67	31.87	32.07	31.87
222	23.99	23.93	24.09	24.26	24.05
400	35.18	34.70	34.99	35.15	34.88
331	28.07	28.15	28.40	28.65	28.37
420	20.80	20.70	20.89	21.08	20.81
224	31.25	31.07	31.39	31.67	31.32
115	24.91	24.74	25.01	25.27	24.93
333	24.91	24.63	24.65	25.15	24.71

relativistic Hartree-Fock free atoms placed in the crystalline lattice. The columns are headed with the exchange potential used in the SCOPW model. From Table III, it can be seen that for higher reflections, the RHF results agree with the results obtained using the Kohn-Sham exchange potential. This good agreement illustrates the well-known general result that the Kohn-Sham wave functions are very good for free-atom calculations. For the low reflections, the RHF results are generally too small in semiconductors. The opposite result applies in metals where the valence charge spreads out. It has been found that Slater's results generally give slightly better agreement with experiment for lower reflections.<sup>26</sup>

#### IV. CONCLUSIONS

This work provides a large amount of information about the band structure of BP. These calculations confirm the experimental measurements of Archer *et al.*,<sup>21</sup> Wang *et al.*,<sup>3</sup> and Fomichev *et al.*<sup>22</sup> which indicate that the band gap is near 2 eV. The theoretical results show that the conduction-band minimum is not at  $X$ , as previously believed, but rather along the  $\Delta$  line at 0.81 of the distance from the  $\Gamma$  to the  $X$  point. These results indicate that the assignment made by Wang *et al.* of their weak reflectivity maximum at 5.0 eV to  $\Gamma_{15c}-\Gamma_{15v}$  is incorrect. This weak maximum is most likely due to  $L_{1c}-L_{3v}$  transitions. This work shows that the main reflectivity maximum, that Wang *et al.* found at 6.9 eV and interpreted as due to  $X$ -point transition, is due to transitions in the outer part of the zone, especially the  $U-K$  region. These calculations provide information on physically interesting quantities for which there is no experimental information. These quantities include the spin-orbit

splitting, effective masses, x-ray form factors, and the effects of hydrostatic pressure on the bands.

These results are based almost completely on first principles with no adjustment to fit experiment. The only experimental datum used is the lattice constant. Correlation is neglected and Slater's exchange approximation is made. In the final analysis, the validity of these results depends upon the applicability of Slater's exchange approximation, the validity of the SCOPW model, and the

convergence of the wave-function expansions. Past experience on many tetrahedral compounds gives us considerable faith in the validity of these results.

#### ACKNOWLEDGMENTS

The author is indebted to Dr. R. N. Euwema for his interest, encouragement, and support of this work. He is also grateful to G. Johnson and G. Schantz for their expert drafting of the figures.

<sup>1</sup>F. V. Williams, in *Preparation of III-V Compounds*, edited by R. K. Willardson and H. L. Goering (Reinhold, New York, 1962), p. 171.

<sup>2</sup>A. Perri, S. La Placa, and B. Post, *Acta Cryst.* **11**, 310 (1958).

<sup>3</sup>C. C. Wang, M. Cardona, and A. G. Fischer, *RCA Rev.* **25**, 159 (1964).

<sup>4</sup>R. J. Stirn, in *Semiconductors and Semimetals*, edited by R. K. Willardson and A. C. Beer (Academic, New York, 1970).

<sup>5</sup>R. N. Euwema, T. C. Collins, D. G. Shankland, and J. S. DeWitt, *Phys. Rev.* **162**, 710 (1967).

<sup>6</sup>D. J. Stukel, R. N. Euwema, T. C. Collins, F. Herman, and R. K. Kortum, *Phys. Rev.* **179**, 740 (1969).

<sup>7</sup>D. J. Stukel and R. N. Euwema, *Phys. Rev.* **188**, 1193 (1969).

<sup>8</sup>D. J. Stukel and R. N. Euwema, *Phys. Rev.* **186**, 756 (1969).

<sup>9</sup>T. C. Collins, D. J. Stukel, and R. N. Euwema, *Phys. Rev. B* **1**, 724 (1970).

<sup>10</sup>D. J. Stukel and R. N. Euwema, *Phys. Rev. B* **1**, 1635 (1970).

<sup>11</sup>D. J. Stukel, R. N. Euwema, T. C. Collins, and V. Smith, *Phys. Rev. B* **1**, 779 (1970).

<sup>12</sup>C. Herring, *Phys. Rev.* **57**, 1169 (1940).

<sup>13</sup>J. C. Slater, *Phys. Rev.* **81**, 385 (1951).

<sup>14</sup>W. Kohn and L. J. Sham, *Phys. Rev.* **140**, A133

(1965).

<sup>15</sup>R. Gaspar, *Acta. Phys. Acad. Sci. Hung.* **3**, 263 (1954).

<sup>16</sup>For a review of this work, the reader can refer to the excellent review article by L. Hedin and S. Lundqvist, in *Solid State Physics*, edited by F. Seitz and D. Turnbull (Academic, New York, to be published).

<sup>17</sup>R. N. Euwema, D. J. Stukel, T. C. Collins, J. S. DeWitt, and D. G. Shankland, *Phys. Rev.* **178**, 1419 (1969).

<sup>18</sup>F. Herman and S. Skillman, in *Proceedings of the International Conference on Semiconductor Physics, Prague, 1960* (Publishing House of Czechoslovak Academy of Science, Prague, 1961), p. 20.

<sup>19</sup>R. N. Euwema and D. J. Stukel, this issue, *Phys. Rev. B* **1**, 4692 (1970).

<sup>20</sup>B. Stone and D. Hill, *Phys. Rev. Letters* **4**, 282 (1960).

<sup>21</sup>R. J. Archer, R. Y. Koyama, E. E. Loebner, and R. C. Lucas, *Phys. Rev. Letters* **12**, 538 (1964).

<sup>22</sup>V. A. Fomichev, I. I. Zhukova, and I. K. Polushina, *J. Phys. Chem. Solids* **29**, 1025 (1968).

<sup>23</sup>P. Manca, *J. Phys. Chem. Solids* **20**, 268 (1961).

<sup>24</sup>N. J. Sclar, *J. Appl. Phys.* **33**, 2999 (1962).

<sup>25</sup>R. J. Stearns, *J. Appl. Phys.* **36**, 330 (1965).

<sup>26</sup>P. M. Raccah, R. N. Euwema, D. J. Stukel, and T. C. Collins, *Phys. Rev. B* **1**, 756 (1970).

## Formation of *I* Centers in LiF under Electron Irradiation\*

Yves Farge†

Laboratory of Atomic and Solid State Physics, Cornell University, Ithaca, New York 14850

(Received 4 February 1970)

The lithium interstitial model (antimorph of the *H* center) for the defect associated with the 5430-Å absorption band formed in LiF by electron or neutron irradiation at 77 °K is strongly supported by new experimental results: The creation rate of these defects is proportional to the incident electron flux, is independent of the *F*-center creation rate, and increases with the thickness of the sample, in good agreement with a knock-on process.